Inorganica Chimica Acta 393 (2012) 261–268

Contents lists available at SciVerse ScienceDirect

Inorganica Chimica Acta

journal homepage: www.elsevier.com/locate/ica

Cyclometalated phenylquinoline rhodium complexes as protein kinase inhibitors

Stefan Mollin, Sebastian Blanck, Klaus Harms, Eric Meggers *

Fachbereich Chemie, Philipps-Universität Marburg, Hans-Meerwein-Straße, 35043 Marburg, Germany

ARTICLE INFO

Article history:
Available online 30 April 2012

Metals in Medicine Special Issue
Dedicated to Prof. James Dabrowiak.

Keywords:
Rhodium
Cyclometalation
Kinase inhibitors
Chiral ligand
Asymmetric synthesis

ABSTRACT

A new metal-containing scaffold for the generation of rhodium(III)-based protein kinase inhibitors is introduced in which the pharmacophore ligand 4-phenylpyrrolo[3,4-*c*]quinoline-1,3(2*H*)-dione is designed to form two hydrogen bonds with the hinge region of the ATP-binding site. The phenylquinoline ligand binds to rhodium(III) in a cyclometalated fashion by coordinating to the quinoline nitrogen and forming a covalent bond to a carbon atom of the phenyl substituent. Additional acyclic tridentate ligands were used to control the relative stereochemistry, whereas a chiral proline-derived tridentate ligand was employed for the asymmetric synthesis of single enantiomers. Finally, protein kinase profiling and inhibition data confirmed that the new rhodium(III)-phenylquinoline scaffold is suitable for the generation of selective protein kinase inhibitors.

1. Introduction

Research from our group over the last several years has demonstrated that substitutionally inert transition metal complexes are sophisticated scaffolds for targeting protein pockets such as enzyme active sites with very high affinities and exquisite selectivities [1,2]. The rich stereochemistry of octahedral metal coordination geometries thereby provides a powerful tool for generating natural-product-like rigid and globular molecular structures that can fill protein pockets in unique fashions [3], as has been demonstrated for the design of octahedral ruthenium [4], iridium [5], and rhodium [6] complexes as highly potent and selective protein kinase inhibitors. Our previously developed metallo-pyridocarbazole scaffold was inspired by the natural product staurosporine and served for the generation of ATP-competitive protein kinase inhibitors by forming two key hydrogen bonds with the hinge region of the ATP binding site (Fig. 1) [2]. Although this design strategy was highly successful, we were seeking new scaffolds for metal-containing protein kinase inhibitors because of the somewhat cumbersome synthesis of the pyridocarbazole heterocycle [7] combined with the expectation that a positioning of the metal at a different position within the ATP-binding site might allow us to discover metal-based inhibitors with hitherto unobserved kinase inhibition properties [8]. In this study, we now introduce such a simplified new design in which cyclometalated rhodium(III) complexes with the pharmacophore ligand 4-phenylpyrrolo[3,4-c]quinoline-1,3(2*H*)-dione are designed to interact with the hinge region of protein kinases (Fig. 1). We furthermore demonstrate that carefully tailored multidentate ligands are ideally suited to control the relative and even absolute metal-centered configuration for the stereoselective synthesis of substitutionally inert rhodium(III) complexes with biological activities.

2. Results and discussion

2.1. Synthesis of 4-phenylpyrrolo[3,4-c]quinoline-1,3(2H)-dione ligands

The ligand 4-phenyl-pyrrolo[3,4-*c*]quinoline-1,3(2*H*)-dione (**1a**) and its benzylated derivative (**1b**) were synthesized according to Scheme 1. The reaction of isatine (**2**) with ethyl benzoylacetate (**3**) under basic conditions afforded through a Pfitzinger reaction the dicarboxylic acid **4** (45%) according to a literature protocol [9]. Next, reaction of **4** with acetic anhydride afforded the anhydride **5**, followed by a reaction with ammonium acetate or benzylamine to obtain the desired ligands **1a** and **1b** in yields of 52% and 78% over two steps, respectively.

2.2. Synthesis of rhodium(III) complexes

Although we were not successful in synthesizing any stable ruthenium complexes with ligands **1a** or **1b**, revealingly, the reaction of **1b** and **1a** with $RhCl_3{\cdot}3H_2O$ in EtOH/H_2O 1:1 at 90 °C for 3 h, followed by the addition of 2-[(pyridin-2-ylmethyl)thio]acetic acid (**6**) and a continued heating for another 16 h afforded the complexes **8** and **9**, respectively, as single diastereomers albeit in somewhat low yields (Scheme 2, Table 1). Other diastereomers could not be isolated although their formation in small amounts cannot be entirely ruled out. In contrast, the reaction of **1a** with $RhCl_3{\cdot}3H_2O$

* Corresponding author. Tel.: +49 6421 2821534; fax: +49 6421 2821535.
E-mail address: meggers@chemie.uni-marburg.de (E. Meggers).

0020-1693/$ - see front matter © 2012 Elsevier B.V. All rights reserved.
http://dx.doi.org/10.1016/j.ica.2012.04.035

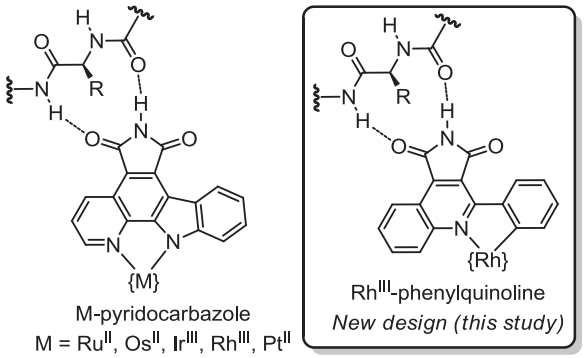

Fig. 1. Previous and new design for metal complexes as protein kinase inhibitors. Shown are the intended interactions of the so-called "pharmacophore chelate ligand" with the hinge region of the ATP-binding site of protein kinases. Note that the imide can hydrogen bond to the hinge region in two different orientations.

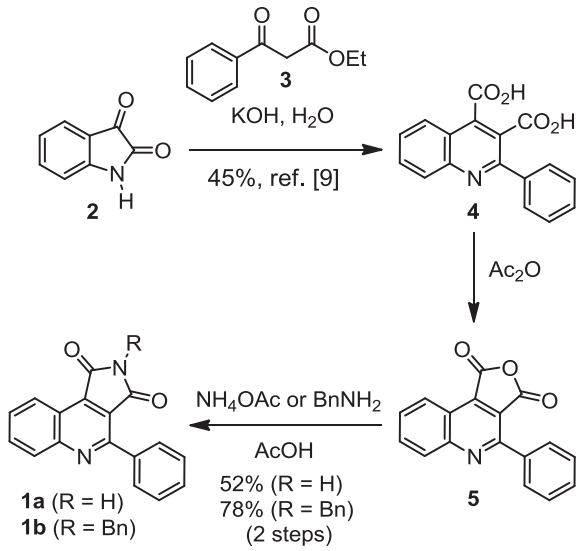

Scheme 1. Synthesis of 4-phenylpyrrolo[3,4-*c*]quinoline-1,3(2*H*)-diones **1a** and **b**.

in EtOH/H_2O 1:1 at 90 °C for 2 h, followed by the addition of 2-[methyl(pyridin-2-ylmethyl)amino]acetic acid (**7**) and a continued heating for another 16 h provided the two diastereomers **10** (10%) and **10′** (21%) which could be separated by silica gel chromatography. The analogous bromide complexes **11** (12%) and **11′** (19%) were obtained when starting from *in situ* generated $RhBr_3$ instead of $RhCl_3$.

Table 1
Synthesis of rhodium complexes **8**–**11**, **10′**, and **11′**.

Complex	R	X	Z	Yield (%)
8	Bn	Cl	S	16
9	H	Cl	S	14
10/**10′**	H	Cl	NCH_3	10/21[a]
11/**11′**	H	Br	NCH_3	12/19[a]

[a] Diastereomers separated by silica gel chromatography.

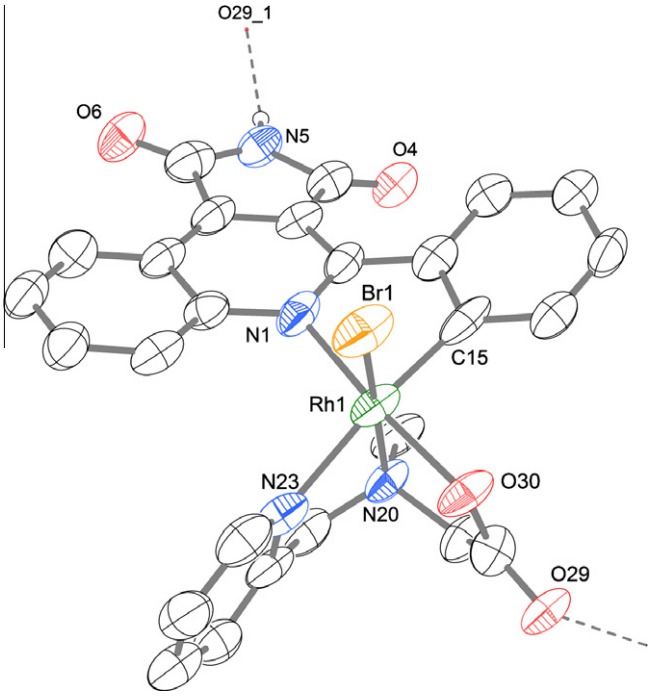

Fig. 2. Crystal structure of rhodium(III) quinoline complex **11**. ORTEP drawing with 50% probability thermal ellipsoids. Selected bond distances (Å) and angles (°): Rh1–C15 = 1.983(13), Rh1–O30 = 2.031(6), Rh1–N1 = 2.077(8), Rh1–N20 = 2.110(8), Rh1–N23 = 2.222(11), Rh1–Br1 = 2.4343(15), C15–Rh1–O30 = 94.1(3), C15–Rh1–N20 = 94.1(4), C15–Rh1–N23 = 173.7(3), C15–Rh1–Br1 = 91.0(3).

A crystal structure of complex **11** is shown in Fig. 2 and confirms the cyclometalation of the phenylquinoline ligand with one formed Rh–C bond (Rh–C = 1.983(13) Å). The phenylquinoline ligand is twisted due to a steric interference between a carbonyl group of the maleimide moiety and a closeby CH-group of the phenyl ring. The tridentate ligand **7** coordinates in a facial fashion and forms in the crystal an intermolecular hydrogen bond between the

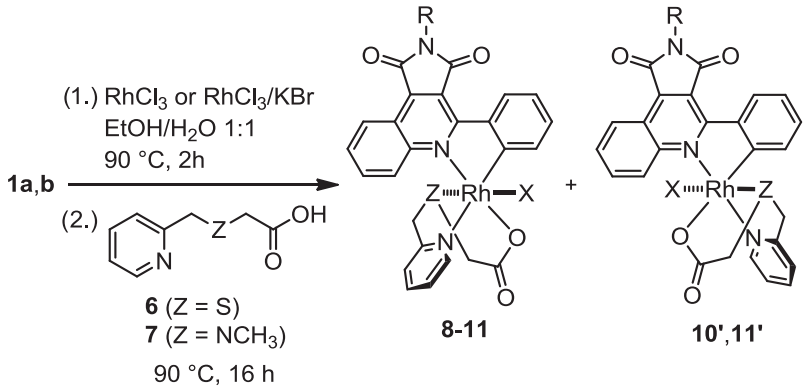

Scheme 2. Synthesis of rhodium quinoline complexes **8**–**11**, **10′**, and **11′**. X = Cl or Br. See Table 1 for more details.

coordinated carboxylate moiety and the imide NH, thus nicely demonstrating the hydrogen donor ability of the maleimide moiety.

2.3. Asymmetric synthesis with chiral ligands

In order to combine the control of relative and absolute metal-centered configuration we employed the chiral proline-based ligands (*S*)-*N*-(pyridin-2-ylmethyl)proline {(*S*)-**12**} and its enantiomer (*R*)-*N*-(pyridin-2-ylmethyl)proline {(*R*)-**12**} [10]. Accordingly, the reaction of **1a** and **1b** first with $RhCl_3 \cdot 3H_2O$, followed by the reaction with (*S*)-**12** provided the complexes Λ-(*S*)-**13a** and Λ-(*S*)-**13b** in an asymmetric fashion as single enantiomers in yields of 31% and 30%, respectively (Scheme 3). As to be expected, the analogous reactions of **1a** and **1b** with $RhCl_3 \cdot 3H_2O$ and the mirror-imaged ligand (*R*)-**12** afforded the enantiomeric complexes Δ-(*R*)-**13a** (30%) and Δ-(*R*)-**13b** (28%), respectively. The absolute configuration of Λ-(*S*)-**13b** was determined by X-ray crystallography (Fig. 3, Table 2) and the remaining compounds were correlated by CD-spectroscopy (Fig. 4). Interestingly, despite the formed Rh–C bond due to cyclometalation of the phenylquinoline ligand, the obtained complexes are surprisingly robust as can be seen in the NMR-experiments shown in Fig. 5 in which no signs of decomposition were detected for complex Δ-(*R*)-**13a** after one week in the presence of millimolar concentrations of the aliphatic thiol β-mercaptoethanol.

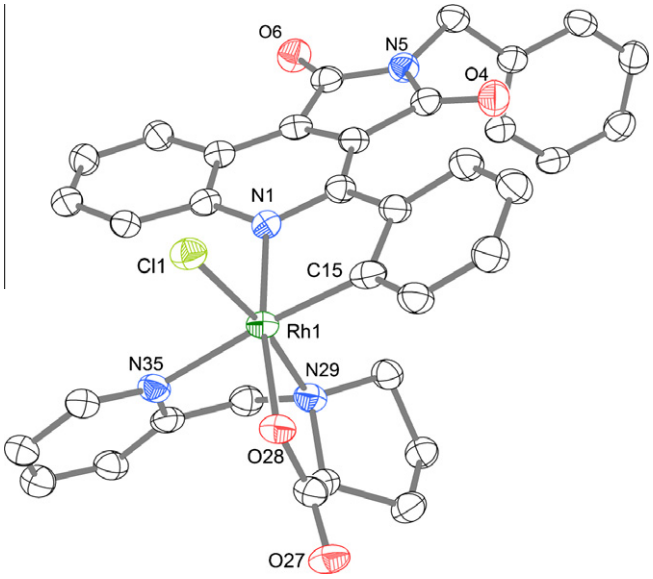

Fig. 3. Crystal structure of enantiomerically pure proline complex Λ-(*S*)-**13b**. Two DMSO solvent molecules are omitted for clarity. ORTEP drawing with 50% probability thermal ellipsoids. Selected bond distances (Å) and angles (°): Rh1–C15 = 1.978(4), Rh1–N1 = 2.065(3), Rh1–N29 = 2.090(3), Rh1–N35 = 2.178(3), Rh1–O28 = 2.029(2), Rh1–Cl1 = 2.3478(9), C15–Rh1–N29 = 97.51(14), O28–Rh1–N29 = 84.10(11), N1–Rh1–N29 = 91.88(12), N29–Rh1–N35 = 78.41(12), N29–Rh1–Cl1 = 171.20(9).

2.4. Protein kinase inhibition

To gain insight into the protein kinase inhibition properties of phenylquinoline rhodium complexes [11], we tested the racemic mixture Λ-(*S*)-**13a**/Δ-(*R*)-**13a** for its protein kinase binding affinity profile against the majority of the human protein kinases encoded in the human genome (human kinome) [12]. This was accomplished by using an active-site-directed competition binding assay with 451 different protein kinases (KINOME*scan*, DiscoveRx) which provides primary data (%ctrl = percent of control: 0% = highest affinity, 100% = no affinity) that correlate with binding constants (K_d) [13]. Interestingly, at a concentration of 10 μM *rac*-**13a**, only a few protein kinases were identified as the main hits with %ctrl values below 60%, namely YSK4 (44%), PKCδ (47%), ZAP70 (50%), MAP3K4 (51%), SRMS (53%), and NEK4 (58%). The human kinase dendrogram shown in Fig. 6 demonstrates that these six kinases are distributed among four protein kinase families.

We selected PKCδ (δ-isoform of protein kinase C) for further investigations. PKCδ belongs to the protein kinase C family of lipid-dependent serine/threonine kinases with a large number of identified PKC isoforms, many of which are critical regulators of diverse cellular functions [14]. The development of specific inhibitors for individual PKC isoforms is therefore of high interest for the development of drugs [15]. Whereas our initial protein kinase profiling was performed with the racemic mixture of **13a**, we determined IC_{50} values (concentration of inhibitor at which the enzyme activity is reduced to 50%) for the individual enantiomers Λ-(*S*)-**13a** and Δ-(*R*)-**13a** against PKCδ at 1 μM ATP as shown in Fig. 7. As to be expected, the IC_{50} differ significantly with Λ-(*S*)-**13a** (IC_{50} = 26 ± 5 μM) being by almost an order of magnitude more potent than the mirror image Δ-(*R*)-**13a** (IC_{50} = 229 ± 42 μM), indicating specific molecular recognition between the chiral active site of PKCδ and Λ-(*S*)-**13a**.

3. Conclusion

We here introduced a new scaffold for rhodium(III) complexes as protein kinase inhibitors which is based on the cyclometalation of 4-phenylpyrrolo[3,4-*c*]quinoline-1,3(2*H*)-dione. Additionally introduced acyclic tridentate ligands were used to control the relative metal-centered configuration, whereas the chiral proline-derived ligands (*S*)- and (*R*)-*N*-(pyridin-2-ylmethyl)proline resulted

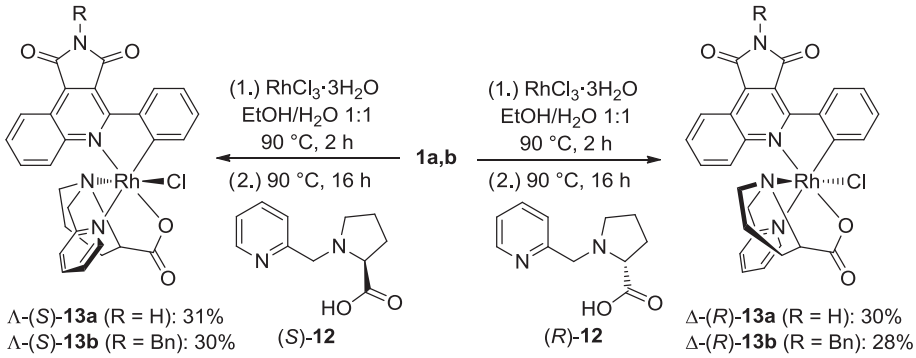

Scheme 3. Asymmetric synthesis of rhodium complexes Λ-(*S*)-**13a**,**b** and Δ-(*R*)-**13a** and **b**.

Table 2
Crystallographic data for rhodium complexes **11** and Λ-(*S*)-**13b**.[a]

	11	Λ-(*S*)-**13b**·2DMSO
Chemical formula	$C_{26}H_{20}BrN_4O_4Rh$	$C_{35}H_{28}ClN_4O_4Rh{\cdot}2(C_2H_6SO)$
M_r	635.28	863.23
Crystal system, space group	monoclinic, $P2_1/c$	orthorhombic, $P2_12_12_1$
a, b, c (Å)	10.559(3), 20.955(3), 11.697(2)	10.1798(3), 11.6800(4), 31.2336(9)
α, β, γ (°)	90, 103.165 (18), 90	90, 90, 90
V (Å^3)	2520.1 (9)	3713.7 (2)
Z	4	4
Radiation type	Mo Kα	Mo Kα
μ (mm^{-1})	2.30	0.70
Crystal size (mm)	0.11 × 0.10 × 0.04	0.31 × 0.10 × 0.04
T_{min}, T_{max}	0.734, 0.974	0.778, 1.100
Number of measured, independent and observed [$I > 2\sigma(I)$] reflections	7730, 4029, 2116	25 884, 7296, 6834
R_{int}	0.091	0.070
$R[F^2 > 2\sigma(F^2)]$, $wR(F^2)$, S	0.063, 0.165, 0.94	0.039, 0.094, 1.03
Number of reflections	4029	7296
Number of parameters	326	483
Number of restraints	0	0
$\Delta\rho_{max}$, $\Delta\rho_{min}$ (e Å^{-3})	0.68, −1.18	0.61, −0.88
Flack parameter (absolute structure)	–	−0.02 (2)
CCDC No.[b]	852553	852554

[a] $R_1 = \Sigma||F_o| - |F_c||/\Sigma|F_o|$; $wR_2 = [w(F_o^2 - F_c^2)^2/\Sigma w(F_o^2)^2]^{1/2}$; $S = \{\Sigma[w(F_o^2 - F_c^2)^2]/(n-p)\}^{1/2}$.
[b] Crystallographic data (excluding structure factors) have been deposited in the Cambridge Crystallographic Data center. CIF files can be obtained from the CCDF free of charge via http://www.ccdc.cam.ac.uk/data_request/cif.

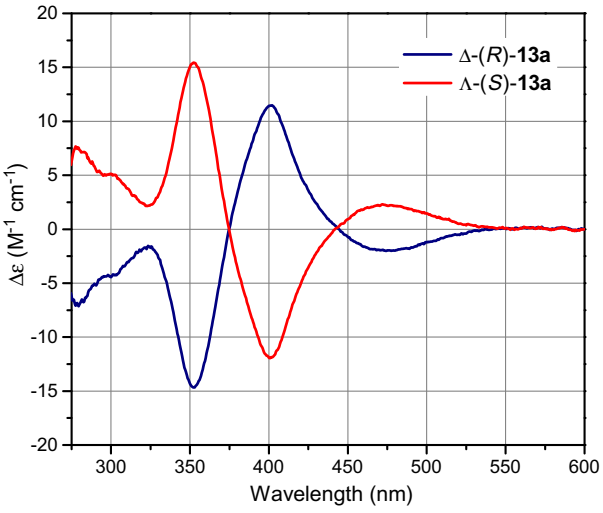

Fig. 4. CD-spectra of the enantiomerically pure rhodium complexes Λ-(*S*)-**13a** (red) and Δ-(*R*)-**13a** (blue) in DMSO. (For interpretation of the references to color in this figure legend, the reader is referred to the web version of this article.)

in the asymmetric synthesis of single enantiomers. Protein kinase profiling and inhibition experiments confirmed that this new rhodium(III)-phenylquinoline scaffold shows promise for the design of inert rhodium(III)-based protein kinase inhibitors. Thus, this work demonstrates that carefully tailored chiral multidentate ligands are ideally suited to control relative and absolute stereochemistry simultaneously for the asymmetric synthesis of substitutionally inert metal complexes with biological activities.

4. Experimental

4.1. Materials and methods

Reactions were carried out using oven-dried glassware and conducted under a positive pressure of nitrogen unless otherwise specified. 2-Phenyl-3,4-dicarboxylic acid (**4**) was synthesized from commercially available isatine (**2**) and ethyl benzoylacetate (**3**) as described in the literature [9]. The ligands 2-[(pyridin-2-ylmethyl)thio]acetic acid, 2-[methyl(pyridin-2-ylmethyl)amino]acetic acid, and (*R*)- plus (*S*)-*N*-(pyridin-2-ylmethyl)proline were synthesized as reported [16,17]. Rhodium(III) chloride trihydrate

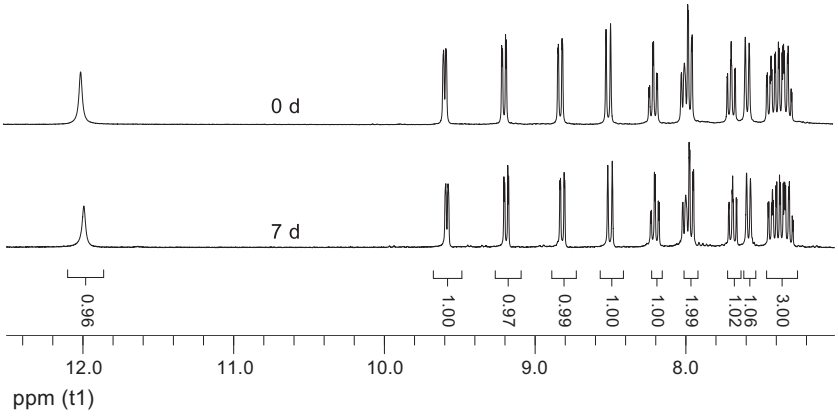

Fig. 5. Stability evaluation of compound Δ-(*R*)-**13a** (8.3 mM) in DMSO-d_6/D_2O 5:1 in the presence of β-mercaptoethanol (4.2 mM). Shown are the aromatic regions of the ^{1}H NMR spectra right after the addition of β-mercaptoethanol (0 day) and after one week (7 days).

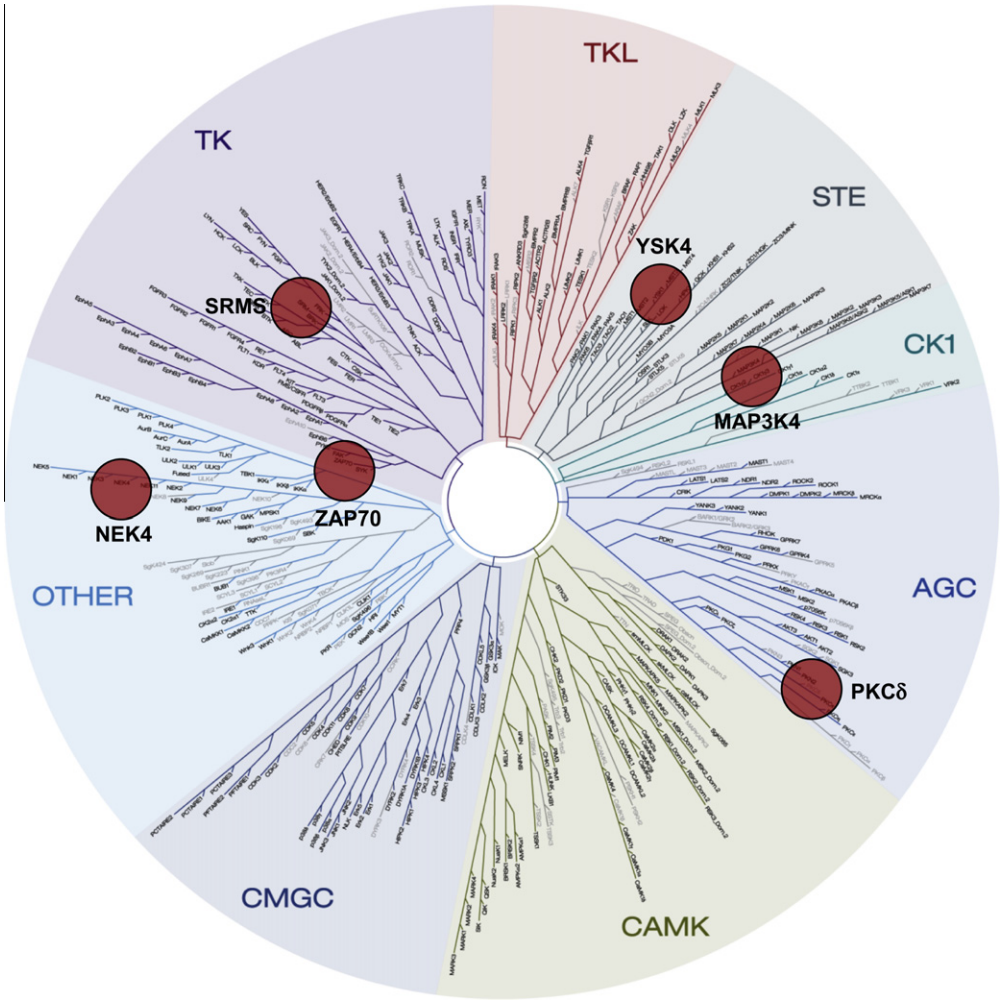

Fig. 6. Protein kinase selectivity of racemic complex **13a** (10 μM) as determined by an active-site-directed affinity screening (KINOME*scan*, DiscoveRx) against 451 human protein kinases. Representation of the main hits (< 60% of control, large red circles) within the human kinase dendrogram which displays the protein kinase families and the evolutionary relationships between the individual kinases. YSK4 = 44%, PKCδ = 47%, ZAP70 = 50%, MAP3K4 = 51%, SRMS = 53%, and NEK4 = 58%.

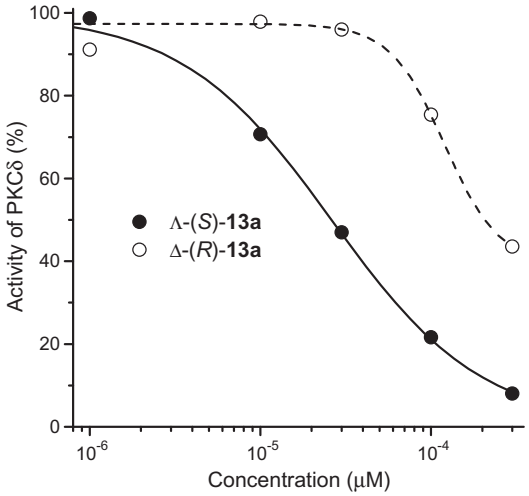

Fig. 7. IC_{50} curves of the two enantiomers Λ-(*S*)-**13a** and Δ-(*R*)-**13a** against PKCδ at ATP concentrations of 1 μM.

and other chemicals as well as all solvents were used as received from standard suppliers. NMR spectra were recorded on an Avance 300 (300 MHz), DRX-400 (400 MHz), or Avance 500 (500 MHz) spectrometer. Infrared spectra were recorded on a Bruker Alpha FTIR. CD spectra were recorded on a JASCO J-810 CD spectropolarimeter with cuvettes of 1 mm pathlength. High resolution mass spectra were obtained with a Finnigan LTQ-FT instrument using either APCI or ESI.

4.2. Compound preparation

4.2.1. 4-Phenylpyrrolo[3,4-c]quinoline-1,3(2H)-dione (**1a**)

A solution of 2-phenyl-3,4-dicarboxylic acid (**4**) (5.87 g, 20.0 mmol) in acetic anhydride (120 mL) was heated to 130 °C for 3 h. During this time the solution gradually changed from yellow to black and the precipitation of a yellow solid was observed. The solvent was removed *in vacuo* and anhydride **5** was obtained which was used immediately for the next step. Anhydride **5** was dissolved in glacial acetic acid (70 mL), ammonium acetate (2.31 g, 30.0 mmol) was added, and the solution was heated to reflux for 16 h. The solvent was removed *in vacuo*, the resulting brown/black solid suspended in ethyl acetate (40 mL) and heated to reflux for 15 min leaving behind a yellow solid. The solid was filtered off, washed with ethyl acetate, and dried *in vacuo* to provide 4-phenylpyrrolo[3,4-*c*]quinoline-1,3(2*H*)-dione (**1a**) as yellow solid (2.85 g, 10.4 mmol, 52%). ^{1}H NMR (300 MHz, DMSO-d_6): δ (ppm) 11.61 (s, 1H), 8.78 (dd, J = 8.3, 0.8 Hz, 1H), 8.19 (d, J = 8.3 Hz, 1H), 8.01–7.92 (m, 3H), 7.86–7.81 (m, 1H), 7.56–7.51 (m, 3H). ^{13}C NMR

(75 MHz, DMSO-d_6): δ (ppm) 169.1, 168.4, 154.4, 150.5, 138.0, 136.7, 132.8, 130.1, 129.52, 129.49, 127.7, 124.3, 122.4, 120.3. IR (film, cm^{-1}): 3185, 3060, 1767, 1708, 1618, 1583, 1351, 1318, 1294, 1082, 1017, 772, 759, 724, 691, 649, 591, 488. HRMS: calcd. for $C_{17}H_{11}N_2O_2$ $(M+H)^+$ 275.0815, found 275.0812.

*4.2.2. 2-Benzyl-4-phenylpyrrolo[3,4-c]quinoline-1,3(2H)-dione (**1b**)*

A solution of 2-phenyl-3,4-dicarboxylic acid (**4**) (5.87 g, 20.0 mmol) in acetic anhydride (120 mL) was heated to 130 °C for 3 h. During this time the solution gradually changed from yellow to black and the precipitation of a yellow solid was observed. The solvent was removed *in vacuo* and anhydride **5** was obtained which was used immediately for the next step. Anhydride **5** was dissolved in glacial acetic acid (70 mL), benzyl amine (3.28 mL, 30.0 mmol) was added, and the solution was heated to 120 °C for 3 h. The solvent was removed *in vacuo*, the resulting brown/black solid suspended in ethyl acetate (40 mL) and heated to reflux for 15 min leaving behind a yellow solid. The solid was filtered off, washed with ethyl acetate, and dried *in vacuo* to provide 2-benzyl-4-phenylpyrrolo[3,4-*c*]quinoline-1,3(2*H*)-dione (**1b**) as yellow powder (5.68 g, 15.6 mmol, 78%). ^{1}H NMR (300 MHz, DMSO-d_6): δ (ppm) 9.81 (d, *J* = 7.6 Hz, 1H), 8.23 (d, *J* = 8.3 Hz, 1H), 8.05–7.99 (m, 1H), 7.97–7.93 (m, 2H), 7.90–7.85 (m, 1H), 7.56–7.53 (m, 3H), 7.41–7.27 (m, 5H), 4.82 (s, 2H). ^{13}C NMR (75 MHz, DMSO-d_6): δ (ppm) 167.6, 167.0, 154.2, 150.6, 137.2, 136.6, 136.4, 133.0, 130.1, 129.7, 129.62, 129.57, 128.5, 127.7, 127.5, 127.4, 124.3, 121.6, 120.1, 41.1. IR (film, cm^{-1}): 3056, 2940, 1705, 1619, 1683, 1553, 1491, 1429, 1390, 1347, 1109, 1069, 922, 775, 752, 696, 651, 626, 497. HRMS: calcd. for $C_{24}H_{17}N_2O_2$ $(M+H)^+$ 365.1285, found 365.1280.

*4.2.3. Complex **8***

A mixture of 2-benzyl-4-phenylpyrrolo[3,4-*c*]quinoline-1,3(2*H*)-dione (**1b**) (14.6 mg, 40.0 μmol) and $RhCl_3{\cdot}3H_2O$ (10.5 mg, 40.0 μmol) in EtOH/H_2O 1:1 (4.0 mL) was refluxed at 90 °C for 2 h. To the resulting dark solution was added 2-[(pyridin-2-ylmethyl)thio]acetic acid (7.3 mg, 40.0 μmol) and the reaction mixture was refluxed at 90 °C for further 16 h. Then, the solvent was removed and the crude material was purified by silica gel chromatography with CH_2Cl_2/MeOH (gradient 50:1 to 20:1). The combined product eluents were dried *in vacuo* to provide complex **8** as yellow solid (4.4 mg, 6.40 μmol, 16%). ^{1}H NMR (300 MHz, DMSO-d_6): δ (ppm) 9.74 (d, *J* = 5.7 Hz, 1H), 9.59 (d, *J* = 8.8 Hz, 1H), 9.14 (dd, *J* = 8.0, 1.4 Hz, 1H), 8.92 (dd, *J* = 8.3, 1.2 Hz, 1H), 8.19 (td, *J* = 7.7, 1.4 Hz, 1H), 8.02–7.96 (m, 1H), 7.93–7.87 (m, 1H), 7.81–7.76 (m, 2H), 7.49–7.46 (m, 2H), 7.40–7.30 (m, 3H) 7.23 (td, *J* = 7.6, 1.2 Hz, 1H), 7.15 (td, *J* = 7.4, 1.5 Hz, 1H), 6.62 (dd, *J* = 7.7, 0.9 Hz, 1H), 4.94 (s, 2H), 4.43 (d, *J* = 17.3 Hz, 1H), 4.40 (d, *J* = 17.4 Hz, 1H), 3.20 (d, *J* = 3.4 Hz, 2H). IR (film, cm^{-1}): 3454, 3108, 3050, 2956, 2141, 1772, 1713, 1622, 1437, 1395, 1348, 1276, 1225, 1169, 1124, 765, 700, 636. HRMS: calcd. for $C_{32}H_{24}ClN_3O_4Rh$ $(M+H)^+$ 684.0226, found 684.0225; calcd. for $C_{32}H_{23}ClN_3O_4RhNa$ $(M+Na)^+$ 706.0045, found 706.0047.

*4.2.4. Complex **9***

A mixture of 4-phenylpyrrolo[3,4-*c*]quinoline-1,3(2*H*)-dione (**1a**) (11.0 mg, 40.0 μmol) and $RhCl_3{\cdot}3H_2O$ (10.5 mg, 40.0 μmol) in EtOH/H_2O 1:1 (4.0 mL) was refluxed at 90 °C for 2 h. To the resulting dark solution was added 2-[(pyridin-2-ylmethyl)thio]acetic acid (7.3 mg, 40.0 μmol) and the reaction mixture was refluxed at 90 °C for further 16 h. Then, the solvent was removed and the crude material was purified by silica gel chromatography with CH_2Cl_2/MeOH (gradient 50:1 to 30:1). The combined product eluents were dried *in vacuo* to provide complex **9** as yellow solid (3.4 mg, 5.73 μmol, 14%). ^{1}H NMR (300 MHz, DMSO-d_6): δ (ppm) 12.04 (bs, 1H), 9.74 (d, *J* = 5.7 Hz, 1H), 9.59 (d, *J* = 8.9 Hz, 1H), 9.16 (dd, *J* = 7.9, 1.2 Hz, 1H), 8.92 (dd, *J* = 8.2, 0.9 Hz, 1H), 8.19 (td, *J* = 7.7, 1.3 Hz, 1H), 8.00–7.94 (m, 1H), 7.91–7.85 (m, 1H), 7.81–7.77 (m, 2H), 7.23 (td, *J* = 7.6, 1.0 Hz, 1H), 7.14 (td, *J* = 7.7, 1.4 Hz, 1H), 6.61 (d, *J* = 7.4 Hz, 1H), 4.44 (d, *J* = 17.4 Hz, 1H), 4.40 (d, *J* = 17.0 Hz, 1H), 3.20 (d, *J* = 16.9 Hz, 1H), 3.17 (d, *J* = 16.3 Hz, 1H). ^{13}C NMR (125 MHz, DMSO-d_6): δ (ppm) 172.6, 168.2, 167.9, 163.3, 162.8 (d, *J* = 26.6 Hz), 161.1, 151.7, 151.1, 144.5, 139.8, 139.3, 133.4, 133.3, 131.9, 131.1, 129.6, 128.5, 124.8, 124.3, 123.4, 122.9, 122.8, 120.6, 54.9, 43.6. IR (film, cm^{-1}) 3414, 3107, 3048, 2966, 2924, 1721, 1601, 1512, 1364, 1312, 1160, 1099, 1030, 769, 627. HRMS: calcd. for $C_{25}H_{18}ClN_3O_4Rh$ $(M+H)^+$ 593.9756, found 593.9756.

*4.2.5. Complexes **10/10′***

A mixture of 4-phenylpyrrolo[3,4-*c*]quinoline-1,3(2*H*)-dione (**1a**) (21.9 mg, 80.0 μmol) and $RhCl_3{\cdot}3H_2O$ (21.1 mg, 80.0 μmol) in EtOH/H_2O 1:1 (8.0 mL) was refluxed at 90 °C for 2 h. To the resulting dark solution was added 2-[methyl(pyridin-2-ylmethyl)amino]acetic acid (14.5 mg, 80.0 μmol) and the reaction mixture was refluxed at 90 °C for further 16 h. Then, the solvent was removed and the crude material was purified by silica gel chromatography with CH_2Cl_2/MeOH (gradient 50:1 to 20:1). The combined product eluents of each stereoisomer were dried *in vacuo* to provide complex **10** as orange solid (4.9 mg, 9.29 μmol, 10%) and complex **10′** as yellow solid (10.1 mg, 17.1 μmol, 21%).

*Complex **10***: ^{1}H NMR (300 MHz, DMSO-d_6): δ (ppm) 11.97 (bs, 1H), 9.55 (d, *J* = 5.2 Hz, 1H), 9.29 (dd, *J* = 7.9, 1.5 Hz, 1H), 8.92 (d, *J* = 8.9 Hz, 1H), 8.86 (dd, *J* = 8.3, 1.1 Hz, 1H), 8.18 (td, *J* = 7.7, 1.6 Hz, 1H), 7.98–7.93 (m, 1H), 7.89 (dd, *J* = 7.6, 1.2 Hz, 1H), 7.73 (td, *J* = 7.6, 0.8 Hz, 1H), 7.64 (d, *J* = 7.7 Hz, 1H), 7.57 (td, *J* = 8.0, 1.5 Hz, 1H), 7.41 (td, *J* = 7.3, 1.5 Hz, 1H), 7.33 (td, *J* = 7.5, 1.4 Hz, 1H), 3.88 (d, *J* = 15.0 Hz, 1H), 3.57 (d, *J* = 14.9 Hz, 1H), 3.09 (d, *J* = 17.0 Hz, 1H), 3.00 (d, *J* = 17.0 Hz, 1H), 1.60 (s, 3H). ^{13}C NMR (125 MHz, DMSO-d_6): δ (ppm) 178.2, 172.9 (d, *J* = 27.1 Hz) 168.3, 168.0, 165.2, 155.4, 151.1, 148.6, 144.8, 140.0, 139.3, 132.9, 132.8, 131.9, 130.2, 129.3, 126.6, 125.8, 125.1, 123.3, 123.2, 122.9, 120.2, 71.3, 66.0, 49.3. IR (film, cm^{-1}): 3413, 3052, 2925, 2855, 2734, 1723, 1643, 1449, 1363, 1311, 1097, 1024, 765, 630, 495. HRMS: calcd. for $C_{26}H_{20}ClN_4O_4RhNa$ $(M+Na)^+$ 613.0120, found 613.0126.

*Complex **10′***: ^{1}H NMR (300 MHz, DMSO-d_6): δ (ppm) 12.01 (bs, 1H), 9.89 (d, *J* = 8.8 Hz, 1H), 9.40 (d, *J* = 5.7 Hz, 1H), 9.29 (dd, *J* = 8.0, 1.3 Hz, 1H), 8.96 (dd, *J* = 8.3, 1.2 Hz, 1H), 8.20 (td, *J* = 7.7, 1.4 Hz, 1H), 8.02–7.96 (m, 1H), 7.93–7.87 (m, 1H), 7.83–7.78 (m, 1H), 7.71 (d, *J* = 7.7 Hz, 1H), 7.24 (td, *J* = 7.7, 1.2, 1H), 7.13 (d, *J* = 7.6 Hz, 1.4 Hz, 1H), 6.72 (dd, *J* = 7.7, 0.8 Hz, 1H), 4.04 (d, *J* = 16.2 Hz, 1H), 3.91 (d, *J* = 16.2 Hz, 1H), 3.05 (s, 2H), 1.66 (s, 3H). ^{13}C NMR (125 MHz, DMSO-d_6): δ (ppm) 173.5, 169.9 (d, *J* = 28.1 Hz) 168.2, 168.0, 163.5, 159.4, 151.2, 149.8, 144.4, 140.0, 139.3, 133.4, 132.0, 130.5, 129.5, 128.0, 125.0, 124.4, 123.0, 122.5, 120.4, 70.7, 69.6, 49.4. IR (film, cm^{-1}): 3409, 3047, 2748, 1721, 1596, 1506, 1449, 1370, 1327, 1099, 1028, 884, 772, 631, 539, 500. HRMS: calcd. for $C_{26}H_{20}ClN_4O_4RhNa$ $(M+Na)^+$ 613.0120, found 613.0125.

*4.2.6. Complexes **11/11′***

A mixture of $RhCl_3{\cdot}3H_2O$ (21.1 mg, 80.0 μmol) and KBr (86.0 mg, 720 μmol) in H_2O (4.0 mL) was heated to 90 °C for 1 h. Then, 4-phenylpyrrolo[3,4-*c*]quinoline-1,3(2*H*)-dione (**1a**, 21.9 mg, 80.0 μmol) and EtOH (8.0 mL) were added to the dark red solution and the mixture was heated to 90 °C for 2 h. To the further darkened solution was added 2-[methyl(pyridin-2-ylmethyl)amino]acetic acid (14.5 mg, 80.0 μmol) and the reaction mixture was refluxed at 90 °C for 16 h. The solvent was removed and the crude material was purified by silica gel chromatography with CH_2Cl_2/MeOH (gradient 50:1 to 20:1). The combined product eluents of each stereoisomer were dried *in vacuo* to provide complex **11** as orange solid

(6.0 mg, 9.44 μmol, 12%) and complex **11′** as yellow solid (9.8 mg, 15.0 μmol, 19%).

*Complex **11***: ^{1}H NMR (300 MHz, DMSO-d_6): δ (ppm) 11.98 (bs, 1H), 9.69 (d, J = 4.6 Hz, 1H), 9.32 (dd, J = 7.9, 1.4 Hz, 1H), 8.92 (d, J = 8.9 Hz, 1H), 8.86 (dd, J = 8.3, 1.1 Hz, 1H), 8.18 (td, J = 7.7, 1.6 Hz, 1H), 7.97–7.93 (m, 1H), 7.88 (dd, J = 7.7, 1.1 Hz, 1H), 7.73 (td, J = 7.6, 0.9 Hz, 1H), 7.64 (d, J = 7.7 Hz, 1H), 7.56 (td, J = 8.0, 1.5 Hz, 1H), 7.40 (td, J = 7.2, 1.5 Hz, 1H), 7.31 (td, J = 7.5, 1.3 Hz, 1H), 3.91 (d, J = 15.0 Hz, 1H), 3.56 (d, J = 14.9 Hz, 1H), 3.09 (d, J = 17.0 Hz, 1H), 2.97 (d, J = 17.0 Hz, 1H), 1.58 (s, 3H). ^{13}C NMR (125 MHz, DMSO-d_6): δ (ppm) 178.6, 172.3 (d, J = 26.1 Hz), 168.3, 168.0, 165.1, 155.5, 151.1, 149.2, 144.7, 140.0, 139.3, 133.2, 132.7, 131.9, 130.2, 129.3, 127.0, 126.0, 125.0, 123.3, 123.1, 120.2, 71.2, 65.6, 49.0. IR (film, cm^{-1}): 3411, 2919, 2852, 2718, 1721, 1605, 1511, 1448, 1370, 1307, 1096, 1023, 890, 761, 629, 495. HRMS: calcd. for $C_{26}H_{20}BrN_4O_4RhNa$ (M+Na)$^+$ 656.9615, found 656.9621.

*Complex **11′***: ^{1}H NMR (300 MHz, DMSO-d_6): δ (ppm) 12.00 (bs, 1H), 9.87 (d, J = 8.6 Hz, 1H), 9.41 (d, J = 5.9 Hz, 1H), 9.29 (dd, J = 7.9, 1.1 Hz, 1H), 8.96 (dd, J = 8.4, 1.2 Hz, 1H), 8.22 (td, J = 7.6, 1.5 Hz, 1H), 8.01–7.96 (m, 1H), 7.92–7.88 (m, 1H), 7.82–7.79 (m, 1H), 7.71 (d, J = 7.6 Hz, 1H), 7.24 (td, J = 7.7, 1.1 Hz, 1H), 7.14 (d, J = 7.7, 1.2 Hz, 1H), 6.72 (dd, J = 7.7, 0.9 Hz, 1H), 4.03 (d, J = 16.5 Hz, 1H), 3.92 (d, J = 16.4 Hz, 1H), 3.05 (s, 2H), 1.65 (s, 3H). ^{13}C NMR (100 MHz, DMSO-d_6): δ (ppm) 174.2, 169.8 (d, J = 27.2 Hz), 168.3, 168.1, 163.7, 159.4, 151.5, 151.4, 144.4, 140.1, 139.4, 133.9, 133.4, 132.1, 130.6, 129.6, 128.4, 125.5, 124.5, 123.2, 123.0, 122.7, 120.5, 70.8, 69.2, 49.1. IR (film, cm^{-1}): 3383, 3051, 2925, 2737, 1769, 1723, 1618, 1509, 1449, 1367, 1310, 1098, 1026, 887, 768, 628, 495. HRMS: calcd. for $C_{26}H_{20}BrN_4O_4RhNa$ (M+Na)$^+$ 656.9615, found 656.9619.

4.2.7. Complex *Λ*-(*S*)-***13a***

A mixture of 4-phenylpyrrolo[3,4-*c*]quinoline-1,3(2*H*)-dione (**1a**; 21.9 mg, 80.0 μmol) and $RhCl_3{\cdot}3H_2O$ (10.5 mg, 80.0 μmol) in EtOH/H_2O 1:1 (8.0 mL) was refluxed at 90 °C for 2 h. To the resulting dark solution was added (*S*)-*N*-(pyridin-2-ylmethyl)proline (18.3 mg, 80.0 μmol) and the reaction mixture was refluxed at 90 °C for further 16 h. Then, the solvent was removed and the crude material was purified by silica gel chromatography with CH_2Cl_2/MeOH (gradient 50:1 to 20:1). The combined product eluents were dried *in vacuo* to provide complex Λ-(*S*)-**13a** as red orange solid (15.3 mg, 24.8 μmol, 31%). ^{1}H NMR (300 MHz, DMSO-d_6): δ (ppm) 11.98 (bs, 1H), 9.57 (d, J = 4.6 Hz, 1H), 9.18 (dd, J = 7.8, 1.5 Hz, 1H), 8.80 (dd, J = 8.4, 1.0 Hz, 1H), 8.49 (d, J = 9.0 Hz, 1H), 8.19 (td, J = 7.7, 1.6 Hz, 1H), 8.00–7.93 (m, 2H), 7.67 (td, J = 7.6, 0.9 Hz, 1H), 7.57 (d, J = 7.7 Hz, 1H), 7.44–7.27 (m, 3H), 3.90 (d, J = 15.2 Hz, 1H), 3.29 (d, J = 15.1 Hz, 1H), 3.07 (dd, J = 9.3, 6.9 Hz, 1H), 2.40–2.32 (m, 1H), 2.21–2.13 (m, 1H), 1.99–1.92 (m, 1H), 1.46–1.30 (m, 2H), 0.85–0.71 (m, 1H). ^{13}C NMR (100 MHz, DMSO-d_6): δ (ppm) 181.7, 174.5 (d, J = 26.4 Hz), 168.4, 168.0, 165.3, 156.3, 150.8, 148.5, 144.3, 139.9, 139.4, 133.9, 132.2, 132.1, 129.3, 129.2, 126.2, 125.8, 125.0, 123.1, 122.7, 120.2, 72.6, 69.4, 58.7, 30.7, 22.9. IR (film, cm^{-1}): 3429, 2051, 2738, 1769, 1722, 1620, 1507, 1447, 1367, 1308, 1272, 1095, 1025, 764, 626, 494. CD (DMSO): Λ, nm ($\Delta\varepsilon$, M^{-1} cm^{-1}) 353 (+15.4), 401 (−11.9), 472 (+2.3). HRMS: calcd. for $C_{28}H_{23}ClN_4O_4Rh$ (M+H)$^+$ 617.0457, found 617.0452; calcd. for $C_{28}H_{22}ClN_4O_4RhNa$ (M+Na)$^+$ 639.0277, found 639.0270.

4.2.8. Complex *Δ*-(*R*)-***13a***

A mixture of 4-phenylpyrrolo[3,4-*c*]quinoline-1,3(2*H*)-dione (**1a**; 21.9 mg, 80.0 μmol) and $RhCl_3{\cdot}3H_2O$ (10.5 mg, 80.0 μmol) in EtOH/H_2O 1:1 (8.0 mL) was refluxed at 90 °C for 2 h. To the resulting dark solution was added (*R*)-*N*-(pyridin-2-ylmethyl)proline (18.3 mg, 80.0 μmol) and the reaction mixture was refluxed at 90 °C for further 16 h. Then, the solvent was removed and the crude material was purified by silica gel chromatography with CH_2Cl_2/MeOH (gradient 50:1 to 20:1). The combined product eluents were dried *in vacuo* to provide complex Δ-(*R*)-**13a** as red orange solid (15.8 mg, 22.4 μmol, 28%).

^{1}H NMR (300 MHz, DMSO-d_6): δ (ppm) 11.98 (bs, 1H), 9.57 (d, J = 4.6 Hz, 1H), 9.18 (dd, J = 7.8, 1.6 Hz, 1H), 8.80 (dd, J = 8.3, 1.1 Hz, 1H), 8.49 (d, J = 9.0 Hz, 1H), 8.19 (td, J = 7.7, 1.6 Hz, 1H), 8.00–7.93 (m, 2H), 7.68 (td, J = 7.7, 0.8 Hz, 1H), 7.57 (d, J = 7.7 Hz, 1H), 7.44–7.27 (m, 3H), 3.89 (d, J = 15.1 Hz, 1H), 3.30 (d, J = 15.1 Hz, 1H), 3.07 (dd, J = 9.3, 6.9 Hz, 1H), 2.40–2.32 (m, 1H), 2.21–2.13 (m, 1H), 2.01–1.89 (m, 1H), 1.46–1.30 (m, 2H), 0.82–0.73 (m, 1H). ^{13}C NMR (100 MHz, DMSO-d_6): δ (ppm) 181.7, 174.5 (d, J = 26.8 Hz), 168.4, 168.0, 165.3, 156.3, 150.8, 148.5, 144.3, 139.9, 139.4, 133.9, 132.2, 132.1, 129.3, 129.2, 126.2, 125.8, 125.0, 123.1, 122.7, 120.2, 72.6, 69.4, 58.7, 30.7, 22.9. IR (film, cm^{-1}): 3426, 3140, 3048, 2923, 2854, 2738, 1770, 1723, 1617, 1507, 1447, 1366, 1306, 1096, 1053, 1025, 766, 494. 639.0271. CD (DMSO): λ, nm ($\Delta\varepsilon$, M^{-1} cm^{-1}): 402 nm (+11.5), 353 nm (−14.7). HRMS: calcd. for $C_{28}H_{23}ClN_4O_4Rh$ (M+H)$^+$ 617.0457, found 617.0454.

4.2.9. Complex *Λ*-(*S*)-***13b***

A mixture of 2-benzyl-4-phenylpyrrolo[3,4-*c*]quinoline-1,3(2*H*)-dione (**1b**; 29.2 mg, 80.0 μmol) and $RhCl_3{\cdot}3H_2O$ (10.5 mg, 80.0 μmol) in EtOH/H_2O 1:1 (8.0 mL) was refluxed at 90 °C for 2 h. To the resulting dark solution was added (*S*)-*N*-(pyridin-2-ylmethyl)proline (18.3 mg, 80.0 μmol) and the reaction mixture was refluxed at 90 °C for further 16 h. The solvent was removed and the crude material was purified by silica gel chromatography with CH_2Cl_2/MeOH (gradient 50:1 to 20:1). The combined product eluents were dried *in vacuo* to provide rhodium complex Λ-(*S*)-**13b** as orange solid (17.0 mg, 24.0 μmol, 30%). ^{1}H NMR (300 MHz, DMSO-d_6): δ (ppm) 9.57 (d, J = 4.8 Hz, 1H), 9.22 (dd, J = 7.8, 1.5 Hz, 1H), 8.83 (dd, J = 8.4, 1.0 Hz, 1H), 8.52 (d, J = 9.0 Hz, 1H), 8.20 (td, J = 7.7, 1.6 Hz, 1H), 8.01–7.94 (m, 2H), 7.70 (td, J = 7.6, 0.9 Hz, 1H), 7.58 (d, J = 7.7 Hz, 1H), 7.50–7.28 (m, 8H), 4.93 (s, 2H), 3.90 (d, J = 15.2 Hz, 1H), 3.33 (d, J = 15.2 Hz, 1H), 3.08 (d, J = 16.2 Hz, 1H), 2.40–2.32 (m, 1H), 2.21–2.13 (m, 1H), 1.99–1.91 (m, 1H), 1.44–1.30 (m, 2H), 0.80–0.71 (m, 1H). IR (film, cm^{-1}): 3458, 3056, 2927, 1773, 1712, 1641, 1583, 1508, 1445, 1396, 1359, 1054, 1027, 764, 636, 502. CD (DMSO): λ, nm ($\Delta\varepsilon$, M^{-1} cm^{-1}) 267 (+8.9), 357 (+10.0), 400 (−3.8). HRMS: calcd. for $C_{35}H_{29}ClN_4O_4Rh$ (M+H)$^+$ 707.0927, found 707.0920.

4.2.10. Complex *Δ*-(*R*)-***13b***

A mixture of 2-benzyl-4-phenylpyrrolo[3,4-*c*]quinoline-1,3(2*H*)-dione (**1b**; 29.2 mg, 80.0 μmol) and $RhCl_3{\cdot}3H_2O$ (10.5 mg, 80.0 μmol) in EtOH/H_2O 1:1 (8.0 mL) was refluxed at 90 °C for 2 h. To the resulting dark solution was added (*R*)-*N*-(pyridin-2-ylmethyl)proline (18.3 mg, 80.0 μmol) and the reaction mixture was refluxed at 90 °C for further 16 h. The solvent was removed and the crude material was purified by silica gel chromatography with CH_2Cl_2/MeOH (gradient 50:1 to 20:1). The combined product eluents were dried *in vacuo* to provide complex Δ-(*R*)-**13b** as orange solid (15.8 mg, 22.4 μmol, 28%). ^{1}H NMR (300 MHz, DMSO-d_6): δ (ppm) 9.57 (d, J = 5.2 Hz, 1H), 9.21 (dd, J = 7.8, 1.5 Hz, 1H), 8.83 (dd, J = 8.4, 1.1 Hz, 1H), 8.52 (d, J = 9.0 Hz, 1H), 8.20 (td, J = 7.7, 1.6 Hz, 1H), 8.01–7.94 (m, 2H), 7.73–7.67 (m, 1H), 7.58 (d, J = 7.7 Hz, 1H), 7.50–7.28 (m, 8H), 4.93 (s, 2H), 3.89 (d, J = 15.2 Hz, 1H), 3.34–3.32 (m, 1H), 3.10–3.04 (m, 1H), 2.40–2.32 (m, 1H), 2.21–2.12 (m, 1H), 1.99–1.92 (m, 1H), 1.46–1.30 (m, 2H), 0.79–0.71 (m, 1H). ^{13}C NMR (125 MHz, DMSO-d_6): δ (ppm) 181.8, 174.6 (d, J = 26.4 Hz), 167.0, 166.6, 164.9, 156.3, 151.1, 148.6, 144.3, 139.5, 139.3, 136.2, 134.0, 132.5, 132.0, 129.5, 129.4, 128.6, 127.9, 127.6, 126.3, 125.9, 125.1, 123.2, 123.1, 121.7, 120.1, 72.7, 69.4, 58.8, 41.6, 30.7, 22.9. IR (film, cm^{-1}): 3410, 3054, 2928, 1709,

1635, 1407, 1437, 1394, 1357, 1314, 1052, 1026, 1002, 762, 732, 699, 635, 500. CD (DMSO): λ, nm ($\Delta\varepsilon$, $M^{-1}\,cm^{-1}$) 267 (−9.3), 357 (−10.4), 400 (+3.9). HRMS: calcd. for $C_{35}H_{29}ClN_4O_4Rh$ $(M+H)^+$ 707.0927, found 707.0918.

4.3. Assays with protein kinases

The protein kinase selectivity profile of the racemic mixture of **13a** at an assay concentration of 10 μM was derived from an active-site-directed affinity screening against 451 human protein kinases (KINOME*scan*, DiscoveRx) [13]. Determination of IC_{50}-values with PKCδ: Various concentrations of the ruthenium complexes Λ-(*S*)-**13a** and Δ-(*R*)-**13a** were incubated at room temperature in 20 mM MOPS, 30 mM $Mg(OAc)_2$, 0.8 μg/μL BSA, 10% DMSO (resulting from the inhibitor stock solution), pH 7.0, in the presence of substrate PKCtide (50 μM), PKC Lipid Activator (purchased from Millipore Scientific), and human PKCδ (2.0 nM) (purchased from Mo Bi Tec). After 30 min, the reaction was initiated by adding ATP to a final concentration of 1 μM and approximately 0.1 μCi/μL $[\gamma\text{-}^{33}P]$ATP. Reactions were performed in a total volume of 25 μL. After 45 min, the reaction was terminated by spotting 15 μL on a circular P81 phosphocellulose paper (2.1 cm diameter, Whatman), followed by washing three times with 0.75% phosphoric acid and once with acetone. The dried P81 papers were transferred to a scintillation vial, 5 mL of scintillation cocktail was added, the counts per minute (CPM) were measured with a Beckmann Coulter™ LS6500 Multi-Purpose Scintillation Counter, and corrected by the background CPM. The IC_{50} values were determined in triplicate from sigmoidal curve fits.

4.4. Single crystal X-ray diffraction studies

Single crystals of complex **11** were obtained upon standing in a mixture of CH_2Cl_2 and MeOH at room temperature for several days. Single crystals of complex Λ-(*S*)-**13b** were obtained from a DMSO solution after several days. The intensity data sets for the complexes **11** and Λ-(*S*)-**13b** were collected at 100 K using a STOE IPDS-2T system with MoKα radiation ($\lambda = 0.71073$ Å). The data were corrected for absorption effects using multi scanned reflections [18]. The crystal of **11** showed strong mosaicity. Therefore the parameters used for the integration of the intensity data led to severe overlap und reduced the completeness of the data set to 90 %. The structures were solved using direct methods {SIR-92 [19] (**11**), SIR2008 [20] (Λ-(*S*)-**13b**)} and refined using the full matrix least squares procedure implemented in SHELX-97 [21]. Hydrogen atoms were included at calculated positions. The absolute structure of Λ-(*S*)-**13b** was determined.

Acknowledgements

We thank the German Research Foundation (DFG Grant No. ME 1805/2-1) and the National Institutes of Health USA (CA114046) for support of this research. S.B. acknowledges a stipend from the Fonds der Chemischen Industrie.

Appendix A. Supplementary material

Supplementary data associated with this article can be found, in the online version, at http://dx.doi.org/10.1016/j.ica.2012.04.035.

References

[1] Metal complexes for medicine and the life sciences: (a) K.H. Thompson, C. Orvig, Science 300 (2003) 936;
(b) W.H. Ang, P.J. Dyson, Eur. J. Inorg. Chem. (2006) 4003;
(c) T.W. Hambley, Dalton Trans. (2007) 4929;
(d) T.W. Hambley, Science 318 (2007) 1392;
(e) A. Mukherjee, P.J. Sadler, Wiley Encycl. Chem. Biol. (2009) 1;
(f) K.L. Haas, K.J. Franz, Chem. Rev. 109 (2009) 4921;
(g) A. Levina, A. Mitra, P.A. Lay, Metallomics 1 (2009) 458;
(h) E.A. Hillard, G. Jaouen, Organometallics 30 (2011) 20;
(i) G. Gasser, I. Ott, N. Metzler-Nolte, J. Med. Chem. 54 (2011) 3.
[2] E. Meggers, G.E. Atilla-Gokcumen, H. Bregman, J. Maksimoska, S.P. Mulcahy, N. Pagano, D.S. Williams, Synlett 8 (2007) 1177.
[3] (a) E. Meggers, Curr. Opin. Chem. Biol. 11 (2007) 287;
(b) E. Meggers, Chem. Commun. (2009) 1001;
(c) C.L. Davies, E.L. Dux, A.-K. Duhme-Klair, Dalton Trans. (2009) 10141.
[4] (a) J. Maksimoska, L. Feng, K. Harms, C. Yi, J. Kissil, R. Marmorstein, E. Meggers, J. Am. Chem. Soc. 130 (2008) 15764;
(b) L. Feng, Y. Geisselbrecht, S. Blanck, A. Wilbuer, G.E. Atilla-Gokcumen, P. Filippakopoulos, K. Kräling, M.A. Celik, K. Harms, J. Maksimoska, R. Marmorstein, G. Frenking, S. Knapp, L.-O. Essen, E. Meggers, J. Am. Chem. Soc. 133 (2011) 5976.
[5] A. Wilbuer, D.H. Vlecken, D.J. Schmitz, K. Kräling, K. Harms, C.P. Bagowski, E. Meggers, Angew. Chem., Int. Ed. 49 (2010) 3839.
[6] S. Dieckmann, R. Riedel, K. Harms, E. Meggers, Eur. J. Inorg. Chem. (2012) 813.
[7] (a) H. Bregman, D.S. Williams, E. Meggers, Synthesis (2005) 1521;
(b) N. Pagano, J. Maksimoska, H. Bregman, D.S. Williams, R.D. Webster, F. Xue, E. Meggers, Org. Biomol. Chem. 5 (2007) 1218.
[8] For different designs of metal-containing protein kinase inhibitors, see: (a) J. Spencer, A.P. Mendham, A.K. Kotha, S.C.W. Richardson, E.A. Hillard, G. Jaouen, L. Male, M.B. Hursthouse, Dalton Trans. (2009) 918;
(b) B. Biersack, M. Zoldakova, K. Effenberger, R. Schobert, Eur. J. Med. Chem. 45 (2010) 1972;
(c) S. Blanck, T Cruchter, A. Vultur, R. Riedel, K. Harms, M. Herlyn, E. Meggers, Organometallics 30 (2011) 4598.
[9] R.F.C. Brown, K.J. Coulston, F.W. Eastwood, M.R. Moffat, Tetrahedron 48 (1992) 7763.
[10] For asymmetric coordination chemistry, see: (a) J.-L. Pierre, Coord. Chem. Rev. 178–180 (1998) 1183;
(b) U. Knof, A. von Zelewsky, Angew. Chem., Int. Ed. 38 (1999) 302;
(c) H. Brunner, Angew. Chem., Int. Ed. 38 (1999) 1194;
(d) P.D. Knight, P. Scott, Coord. Chem. Rev. 242 (2003) 125;
(e) C. Ganter, Chem. Soc. Rev. 32 (2003) 130;
(f) J. Lacour, V. Hebbe-Viton, Chem. Soc. Rev. 32 (2003) 373;
(g) H. Amouri, M. Gruselle, Chirality in Transition Metal Chemistry: Molecules, Supramolecular Assemblies and Materials, Wiley, 2008;
(h) E. Meggers, Chem. Eur. J. 16 (2010) 752;
(i) E. Meggers, Eur. J. Inorg. Chem. (2011) 2911.
[11] For rhodium complexes with biological activities, see: (a) B. Weber, A. Serafin, J. Michie, C. van Rensburg, J.C. Swarts, L. Böhm, Anticancer Res. 24 (2004) 763;
(b) A. Dorcier, W.H. Ang, S. Bolano, L. Gonsalvi, L. Juillerat-Jeannerat, G. Laurenczy, M. Peruzzini, A.D. Phillips, F. Zanobini, P.J. Dyson, Organometallics 25 (2006) 4090;
(c) A.M. Angeles-Boza, H.T. Chifotides, J.D. Aguirre, A. Chouai, P.K.-L. Fu, K.R. Dunbar, C. Turro, J. Med. Chem. 49 (2006) 6841;
(d) A. Dorcier, C.G. Hartinger, R. Scopelliti, R.H. Fish, B.K. Keppler, P.J. Dyson, J. Inorg. Biochem. 102 (2008) 1066;
(e) M.A. Scharwitz, I. Ott, Y. Geldmacher, R. Gust, W.S. Sheldrick, J. Organomet. Chem. 693 (2008) 2299;
(f) J.D. Aguirre, A.M. Angeles-Boza, A. Chouai, C. Turro, J.-P. Pellois, K.R. Dunbar, Dalton Trans. (2009) 10806;
(g) R. Bieda, M. Dobroschke, A. Triller, I. Ott, M. Spehr, R. Gust, A. Prokop, W.S. Sheldrick, ChemMedChem 5 (2010) 1123;
(h) Y. Geldmacher, R. Rubbiani, P. Wefelmeier, A. Prokop, I. Ott, W.S. Sheldrick, J. Organomet. Chem. 696 (2011) 1023.
[12] G. Manning, D.B. Whyte, R. Martinez, T. Hunter, S. Sudarsanam, Science 298 (2002) 1912.
[13] (a) M.A. Fabian, W.H. Biggs III, D.K. Treiber, C.E. Atteridge, M.D. Azimoara, M.G. Benedetti, T.A. Carter, P. Ciceri, P.T. Edeen, M. Floyd, J.M. Ford, M. Galvin, J.L. Gerlach, R.M. Grotzfeld, S. Herrgard, D.E. Insko, A.G. Lai, J.-M. Lélias, S.A. Mehta, Z.V. Milanov, A.M. Velasco, L.M. Wodicka, H.K. Patel, P.P. Zarrinkar, D.J. Lockhardt, Nat. Biotechnol. 23 (2005) 329;
(b) M.W. Karaman, S. Herrgard, D.K. Treiber, P. Gallant, C.E. Atteridge, B.T. Campbell, K.W. Chan, P. Ciceri, M.I. Davis, P.T. Edeen, R. Faraoni, M. Floyd, J.P. Hunt, D.J. Lockhardt, Z.V. Milanov, M.J. Morrison, G. Pallares, H.K. Patel, S. Pritchard, L.M. Wodicka, P.P. Zarrinkar, Nat. Biotechnol. 26 (2008) 127.
[14] M.E. Reyland, Biochem. Soc. Trans. 35 (2007) 1001.
[15] M. Serova, A. Ghoul, K.A. Benhadji, E. Cvitkovic, S. Faivre, F. Calvo, F. Lokiec, E. Raymond, Sem. Oncol. 33 (2006) 466.
[16] C. Incarvito, A.L. Rheingold, A.L. Gavrilova, C.J. Qin, B. Bosnich, Inorg. Chem. 40 (2001) 4101.
[17] S. Paria, P. Halder, T.K. Paine, Inorg. Chem. 49 (2010) 4518.
[18] A.L. Spek, PLATON, A Multipurpose Crystallographic Tool, Utrecht University, Utrecht, The Netherlands, 1998.
[19] A. Altomare, G. Cascarano, C. Giacovazzo, A. Guagliardi, J. Appl. Crystallogr. 26 (1993) 343.
[20] M.C. Burla, R. Caliandro, M. Camalli, B. Carrozzini, G.L. Cascarano, L. De Caro, C. Giacovazzo, G. Polidori, D. Siliqi, R. Spagna, J. Appl. Crystallogr. 40 (2007) 609.
[21] G.M. Sheldrick, Acta Crystallogr., Sect. A 64 (2008) 112.